



HAL
open science

Experimental Analysis of Unreinforced Masonry Buildings Through the Quasi-Static Test: A Half-Scale Two-Story Modern Masonry Building

Abide Aşıkoğlu, Alberto Barontini, Nathanaël Savalle, Graça Vasconcelos,
Paulo B Lourenço

► To cite this version:

Abide Aşıkoğlu, Alberto Barontini, Nathanaël Savalle, Graça Vasconcelos, Paulo B Lourenço. Experimental Analysis of Unreinforced Masonry Buildings Through the Quasi-Static Test: A Half-Scale Two-Story Modern Masonry Building. North American Masonry Conference, Jun 2023, Omaha, United States. hal-04481902

HAL Id: hal-04481902

<https://hal.science/hal-04481902>

Submitted on 29 Feb 2024

HAL is a multi-disciplinary open access archive for the deposit and dissemination of scientific research documents, whether they are published or not. The documents may come from teaching and research institutions in France or abroad, or from public or private research centers.

L'archive ouverte pluridisciplinaire **HAL**, est destinée au dépôt et à la diffusion de documents scientifiques de niveau recherche, publiés ou non, émanant des établissements d'enseignement et de recherche français ou étrangers, des laboratoires publics ou privés.

Experimental analysis of unreinforced masonry buildings through the quasi-static test: A half-scale two-story modern masonry building

Abide Aşıkoğlu ^{a*}, Alberto Barontini ^a, Nathanael Savalle ^b, Graça Vasconcelos ^a, and Paulo B. Lourenço ^a

a ISISE, Department of Civil Engineering, University of Minho

b Université Clermont Auvergne, Clermont Auvergne INP, CNRS, Institut Pascal, F-63000

Clermont–Ferrand, France

(**corresponding author*)

Abstract:

Masonry is one of the most used construction materials for structural and non-structural elements. The number of masonry constructions is still remarkable in countries where the costs of modern technology are high, as masonry solutions remain the most convenient and economical alternatives. Among these countries, unreinforced masonry is usually found in low- and mid-rise buildings, both residential and commercial. Developed countries, however, have favored alternative construction materials like reinforced concrete and steel, while masonry is regarded as an aesthetic and non-structural feature. Most objections to masonry construction are based on its lack of seismic performance. However, a substantial number of well-preserved masonry structures demonstrate that when they are built properly, they can withstand any form of loading, such as wind or seismic loads. Thus, masonry buildings' seismic performance is underrated and experimental research is necessary to gain insight into their response. The studies available in the literature mainly focus on shake table testing of masonry buildings, while they have not been extensively studied in a quasi-static regimen. In this context, a half-scale two-story unreinforced masonry building with plan irregularity has been tested at the Laboratory of the Structures at the University of Minho. The experimental campaign involves cyclic quasi-static testing with a mode proportional unidirectional loading. Dynamic identification and digital image correlation techniques have been employed to monitor the damage progression. The test has resulted in a rocking response under lateral loading, with a wall detachment from the foundation and slab in the first and second levels, respectively. This paper presents and discusses the experimental procedure and the main outcomes of the study.

Keywords: Unreinforced masonry, Structural irregularity, Quasi-static test, Digital image correlation, Dynamic identification

1 Introduction

Masonry is the very first man-made building material in history, and it has been the keystone of structural engineering for many decades. Naturally available materials inspired its composition and have been applied in different forms, such as adobe, stone, brick, or block, over centuries as building materials. Masonry can be constructed in incremental ways, from a simple brick unit to an architectural masterpiece. Today, a significant number of well-preserved old masonry buildings constitute a considerable portion of the building stock all over the world including regions with high seismicity (Jaiswal and Wald 2008). With the industrial developments, alternative construction solutions, such as reinforced concrete and steel, have been favored among the community, and the number of masonry construction has reduced significantly. Yet, there are several countries where unreinforced masonry (URM) still keeps relevance in the construction market, and it is usually found in low- and mid-rise residential or commercial buildings (Lourenço and Marques 2020).

There is a significant amount of research performed on existing masonry buildings to improve their behavior and extend their life span (Tomažević, M., Lutman, M., & Weiss 1996; Dolce et al. 2008; Mazzon et al. 2009; Mendes 2012; Magenes et al. 2014; Candeias et al. 2017; Graziotti et al. 2017; Kallioras et al. 2018). However, modern unreinforced masonry still requires promotion and further investigations to prove its reasonable structural response, particularly under seismic actions. To what concerns modern constructions, architectural aesthetics play a crucial role in the design process. In particular, unreinforced masonry building design is mainly controlled by architectural aspects in which the elements serve as both architectural and structural components. This eventually leads to designs that usually have irregular structural layouts due to functional, economical, and architectural concerns. From an engineering point of view, the design code discourages irregular structural systems because they increase the seismic vulnerability of buildings (Drysdale and Hamid 2008). However, this approach may not be practical due to the aforementioned reasons. Therefore, it is necessary to understand buildings with irregular structural layouts and optimise their behavior instead of disregarding them.

The present research intends to evaluate the seismic behavior of modern masonry buildings with structural irregularity, which currently lacks investigations, through an experimental campaign. With this aim, cyclic quasi-static testing has been performed on a half-scale unreinforced masonry building. The experimental building has been chosen based on the model tested on a shake table by Avila et al. (2018). The structural irregularity was introduced in the plan as a setback in one corner. In this study, quasi-static testing was preferred because there are various shake table tests available in the literature while quasi-static testing is limited (Magenes et al. 1995, 2014; Tomažević, M., Lutman, M., & Weiss 1996; Dolce et al. 2008; Mazzon et al. 2009; Mendes 2012; Shahzada et al. 2012; Aldemir et al. 2017; Candeias et al. 2017; Graziotti et al. 2017; Kallioras et al. 2018). Another essential aspect of quasi-static testing is that, in practice, nonlinear static analysis is preferred owing to its ease of use (Caddemi et al. 2017; Azizi 2018; Aşıkoğlu et al. 2020). Several commercial programs, which mainly adopt pushover analysis, are developed particularly for masonry buildings and they are used significantly among the engineering community (Lagomarsino et al. 2006; Calì et al. 2012). Therefore, the outcomes of the present experimental campaign provide further knowledge of the quasi-static behavior of these buildings that can be transferred to the practice straightforwardly. In addition to quasi-static testing, the modal properties of the structure were extracted through dynamic identification. Last, but not least, Digital Image Correlation (DIC) was performed to monitor the strains of one of the façades. Finally, the valuable plethora of monitored data brings a comprehensive validation framework for the aforementioned numerical methods in the case of irregular masonry buildings.

2 Building Prototype and Test Setup

The experimental model has been designed to represent typical residential Portuguese houses. The experimental building is irregular in the plan with a setback on one corner. The half-scale two-story URM building has a plan dimension of 419 cm x 368 cm with an inter-story height of 152 cm, as shown in Figure 1. The box behavior is ensured by a 10-cm thick reinforced concrete slab. The building was composed of vertically perforated masonry clay bricks which are available in the market. To ensure interlocking at the corners, masonry units have been assembled following a running bond pattern. The dimensions of masonry clay bricks are 24.5 cm x 10.8 cm x 9.8 cm which is consistent with the chosen scale factor. As per Eurocode 6 (2018), the masonry clay brick is classified as Group 3 having a compressive strength of a minimum of 15 MPa. Furthermore, class M10 ready-mixed mortar has been chosen for bed and head joints.

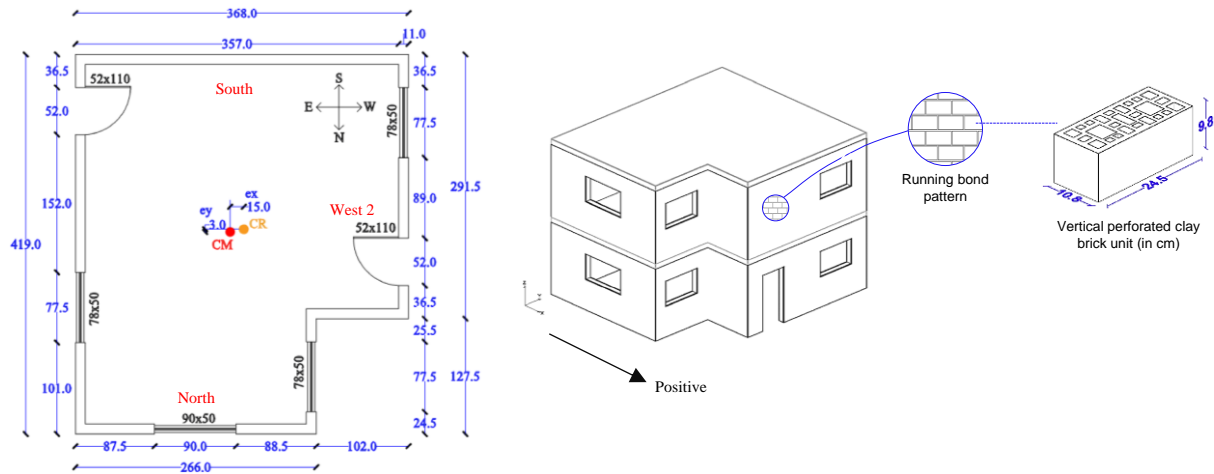
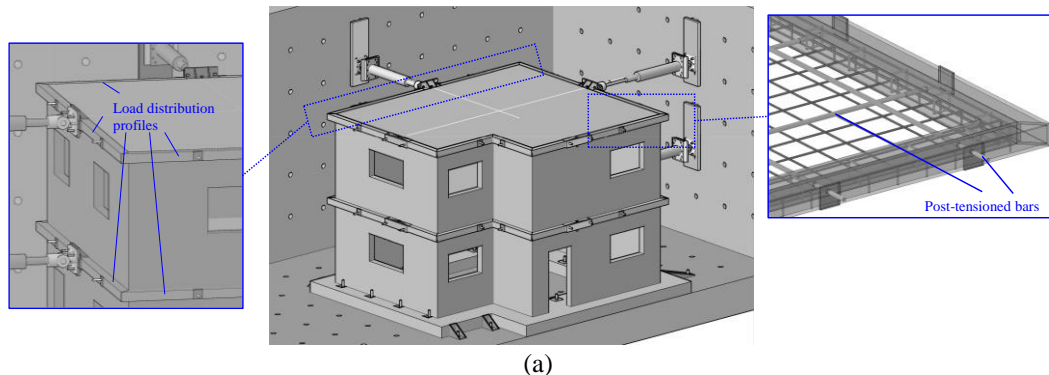


Figure 1. Geometric details and axonometric view of the experimental building (in cm)

The loading application was a major factor controlling the design of the experimental setup. Two 300 kN hydraulic jacks have been positioned at the center of mass of each story/slab (first floor and roof) and connected to steel profiles that aimed to distribute the force to avoid concentrated load application, as shown in Figure 2. These steel profiles have been installed along the perimeter of the structure, and they have been connected with post-tensioned bars. Its main purpose was to maintain the load distribution and avoid the detachment of the steel profiles from the slab during the pulling and pushing of the structure. Hence, the cyclic load was applied through loading and reloading plates, which were also connected with post-tensioned bars inside the RC slab, as illustrated in Figure 2 (b).



(a)

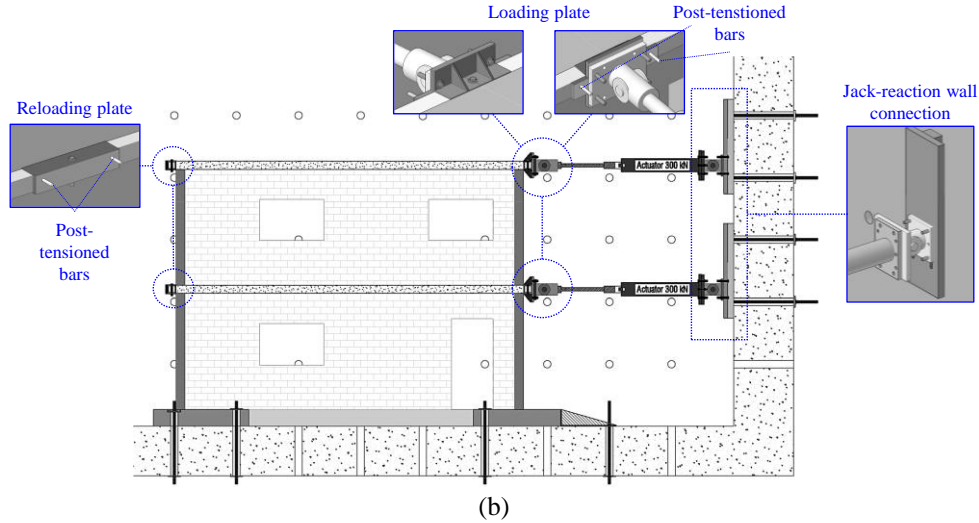


Figure 2. Configuration and details of the experimental setup, (a) 3D view, (b) section view

3 Experimental Program

Within the scope of the project, the experimental campaign is composed of two main parts: material characterization of the masonry and quasi-static testing on a half-scale building. Material characterization tests were developed in Aşıkoglu et al. (2021). In the present paper, quasi-static testing is presented. Additionally, dynamic identification of the experimental building and digital image correlation (DIC) have been carried out to acquire the modal properties and damage evolution of the building, respectively. This section presents instrumentation devices and their layout, and the derivation of the loading protocol.

3.1 Instrumentation

To monitor and measure the building's response, the study building has been equipped with three different devices, namely Linear Variable Differential Transformers (LVDT), accelerometers, and a camera for DIC. A set of LVDTs has been placed on the building aiming at measuring local deformation, while a set of others were installed on external reference frames to monitor the global behavior at specific points. The accelerometers have been mounted on the building to obtain the dynamic properties of the building. Moreover, a camera has been located in front of the North façade to capture the deformations on this façade through the DIC method. Accordingly, a set of LVDTs has been placed at various locations within the building to obtain local and global deformations, as illustrated in Figure 3. This has been achieved by installing a total of 39 LVDTs, which were categorized into four groups based on the deformation types that were measured, including (a) shear (16), (b) lateral (17), (c) uplift (3), and (d) sliding (3).

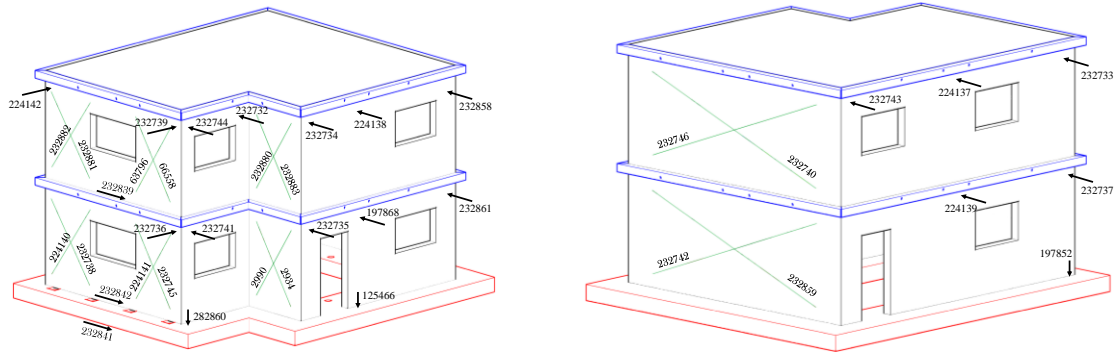


Figure 3. Configuration of the LVDT equipment

In the present study, the Output-Only technique, namely Operational Modal Analysis (OMA), has been adopted to identify the dynamic properties of the tested building. First, the dynamic response of the building has been recorded through accelerometers utilizing ambient vibrations as a source of excitation. Uniaxial accelerometers with high sensitivity (10V/g, 8g resolution and frequency range from 0.15Hz to 1000Hz) have been located at numerous positions and orientations (Figure 4). Their positions have been defined according to the expected vibration modes of the structure estimated through eigenvalue analysis. Given the high number of locations, different acquisition with different setups have been conducted. In total, eight setups have been used, each of them composed of eight accelerometers. To ensure comparable outcomes between the different acquisitions, two locations have been considered as reference points and have been included in all setups (Figure 4). Each acquisition lasted 20 minutes to ensure enough precision in the low-frequency range. The acquired data has been then used to perform OMA using Subspace Stochastic Identification – Unweighted Principal Component (SSI-UPC), and experimental modal parameters (modal frequencies and modal shapes) have been derived.

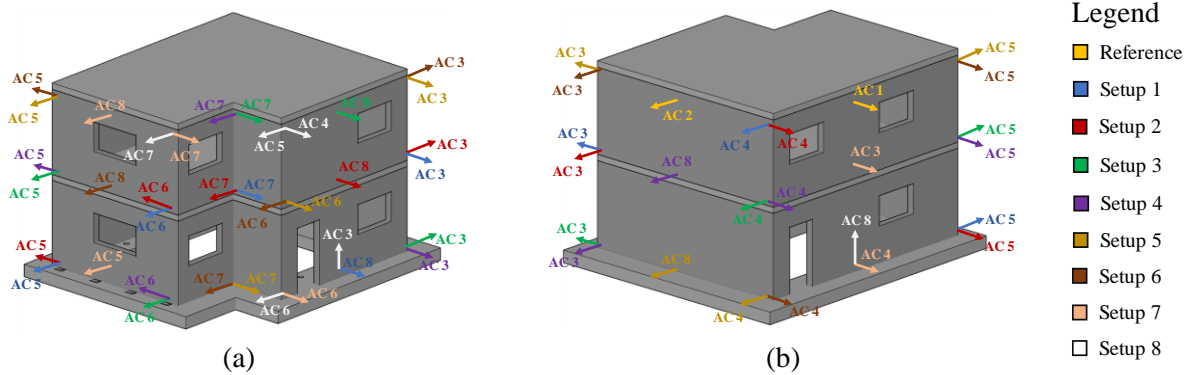


Figure 4. Setup layout and sensor directions for AVM

DIC has become widely used in engineering to monitor material and structural response because of its inexpensive equipment needs, wide full-field measurement, and ease of use. Several studies on masonry, such as Ghiassi et al. (2013), Ghorbani et al. (2015), and Rajaram et al. (2017), used the DIC method to acquire full-field information on displacement, deformation, and crack propagation and demonstrated its potential for providing valuable results. Thus, the North façade, where the first cracks were expected, has been monitored through the DIC technique. Firstly, a random pattern of dots has been sprayed with black paint on the façade, preliminarily painted in white to improve the contrast (Figure 5). Then, a unique camera was located approximately four meters in front of the façade to ensure that the camera captured the entire

building. A Sony DSC-RX100M7 camera of 20 Megapixels (5472x3648) using the manual focus has been fixed on a tripod: the diaphragm opening, shutter speed, and ISO value have then been optimized to obtain enough contrast and light in the pictures. Finally, the pictures have been recorded with a constant frequency of 0.125 Hz (i.e. one picture every eight seconds).



Figure 5. Building façade that DIC was applied

3.2 Loading Protocol

It is noticed that there is a lack of information on how to derive a loading strategy for quasi-static testing on scaled masonry prototypes. Therefore, the authors proposed a loading protocol intended to reproduce a mode-proportional pushover loading. Therefore, it required that the ratio of forces applied by the two hydraulic jacks is constant. A force-controlled loading protocol has been preferred as preliminary trials with a displacement-controlled strategy resulted in an uncontrollable system (in terms of forces). In addition, both the final capacity and stiffness of the structure is unknown, which makes the applicability of a displacement-controlled strategy more complex.

In this study, the loading protocol was derived based on the first dominant mode shape of the building in the transversal direction. Thus, the structural system was simplified in two steps. The first step consists of converting the building from a multi-degree-of-freedom (MDOF) system to a single-degree-of-freedom (SDOF) system by using the building's period from the dynamic identification (Figure 6). The equivalent stiffness of the SDOF system was then calculated by utilizing the period function (Equation 1), in which the period of the system was obtained from the dynamic identification, and the equivalent mass was known.

$$T = 2\pi \sqrt{\frac{m}{k}} \quad (1)$$

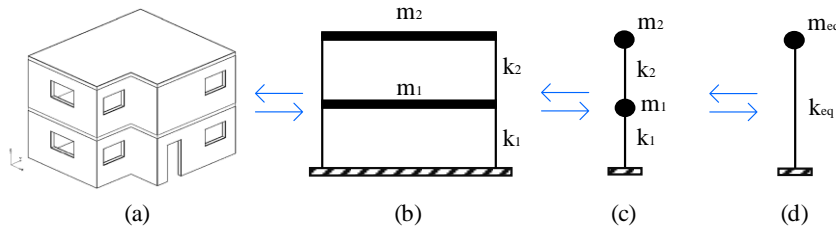


Figure 6. Substitute structural approach, (a) detailed structure, (b) simplified model, (c) 2 DOFs system, (d) SDOF system

In the second step, it has been assumed that a 2-DOF system can be acquired from the SDOF system which has equivalent stiffness (k_{eq}), and it is the equivalence of two springs connected in series. The stiffness at each level has been computed by assuming the stiffness (k_1 and k_2) and mass (m_1 and m_2) at each DOF are equal ($k_1=k_2$, $m_1=m_2$) and, therefore, the stiffness and mass matrix for the 2 DOF system is obtained. Then, the eigenvalue analysis has been computed for the 2 DOF system, and the eigenvectors have been obtained. The normalized eigenvectors have been used to define the load pattern. It is found that the force at the top level is equal to 1 unit while in the first level 0.6 unit of force is needed. At each cycle, the same relation has been used. Figure 7 presents the loading protocol that has been used for the cyclic quasi-static test in terms of total base shear force (sum of the forces applied at the two floors) and base shear coefficient (in relation to the total weight of the structure). Due to the limitations of the equipment, the loading at each level has been applied stepwise, meaning that loading has been employed to one level at a time.

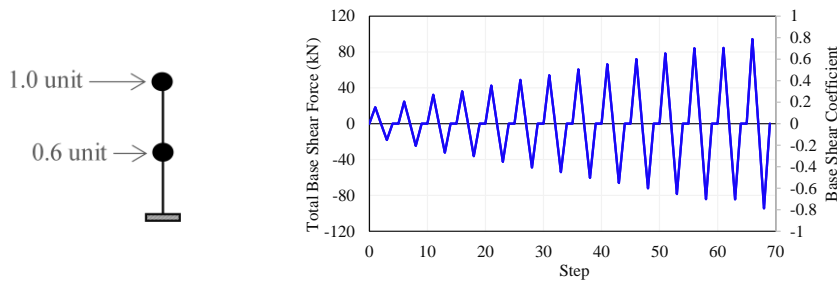


Figure 7. Applied loading protocol in force control

4 Results

In this section, results of operational modal analysis, cyclic quasi-static testing, and DIC are gathered and discussed. The operational modal analysis has been performed by processing the information obtained from ambient vibration measurements in the ARTeMIS Modal program. More specifically, the modal identification process has been carried out using the SSI-UPC (Figure 8). It is found that the first mode is associated with translational movement in the longitudinal direction of the building with a frequency value of 23.9 Hz. The second vibration mode is translational in the transverse direction (25.3 Hz), while a torsional mode is observed as the third mode (39.5 Hz).

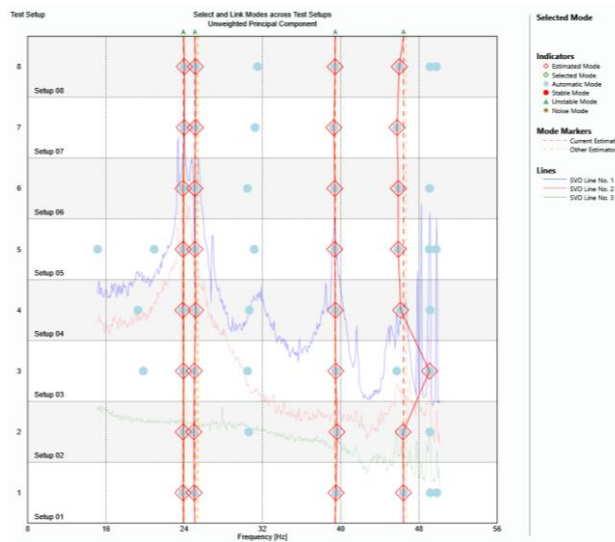


Figure 8. Selection and linking process of modes across all test setups by utilizing the SSI-UPC method

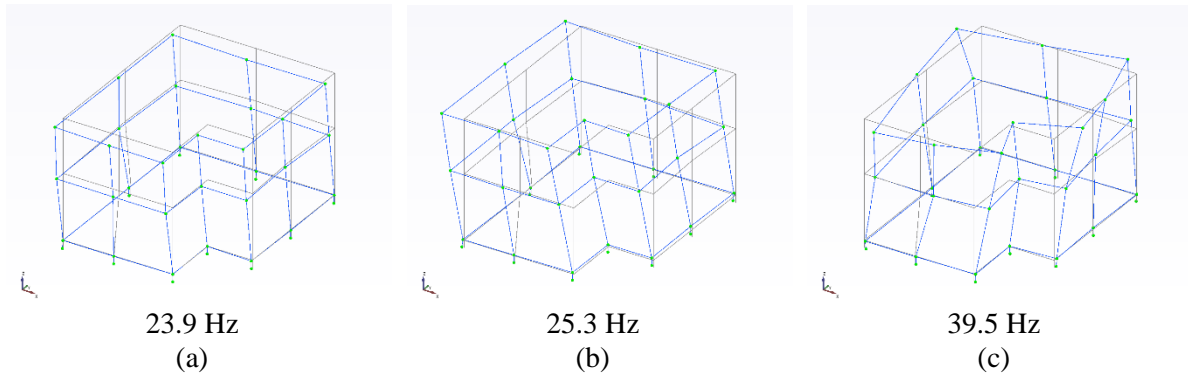


Figure 9. Mode shapes and frequencies of the experimental building, (a) 1st mode, (b) 2nd mode, and (c) 3rd mode

The building's lateral capacity is evaluated in terms of base shear force and lateral displacement. The base shear coefficient has been calculated as the ratio of the total base shear force to the structure's entire weight. The drift, which is the ratio of top displacement to building height, is also monitored. Figure 10 shows the capacity diagrams for each cycle of Figure 7 and the backbone curve at two points. At the top level, LVDT 224138, directly beneath the reloading plate, has been chosen to plot the capacity diagram. This point corresponds to the load application point (in the same direction) and monitors the out-of-plane response of the wall. It was discovered that the structure has a similar level of load in both positive and negative directions in terms of lateral load capacity, which is 75% of the total structural weight (nearly 90 kN). LVDT 232744 is also selected as a control point, as it gives the in-plane response of the masonry façade (Figure 10). According to the preliminary numerical analysis, this point exhibits the largest displacements in the transverse direction. Yet, it is observed that the deformation capacity at both control nodes appears to be similar, proving the box behavior. Furthermore, the top drifts are substantially higher in the negative load direction, nearly 0.09% (i.e. a horizontal displacement equal to 0.0009 times the height of the structure), which could be attributed to the structure uplifting in this direction. The highest drift, on the other hand, is obtained at 0.05% (with a max value of 1.5 mm displacement) in the positive direction. It should be noted that the test was carried out up to the building's maximum lateral load capacity since the loading has been administered in force-controlled mode. As a result, post-peak behavior was not obtained.

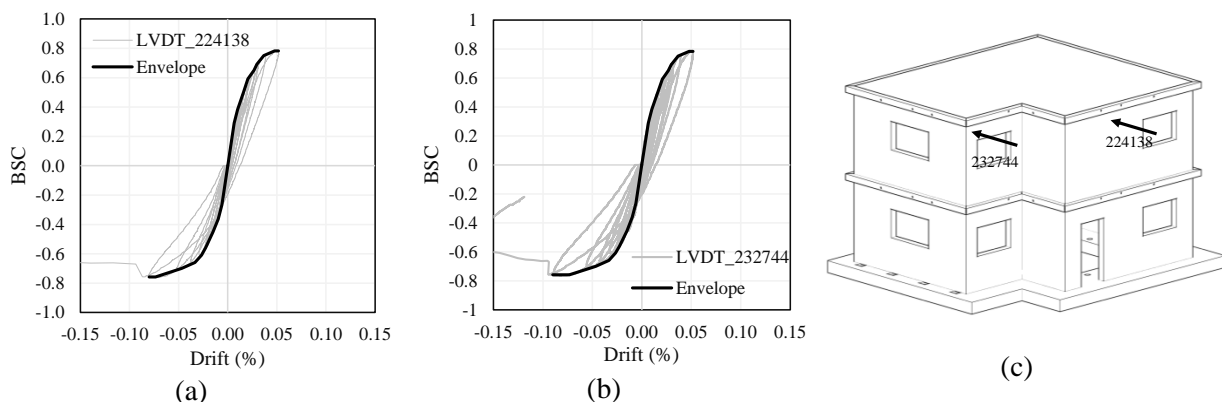


Figure 10. Capacity diagram two control points, (a) LVDT 224138, (b) LVDT 232744, (c) location of the control points

Nevertheless, such experimental results can still be compared to seismic design recommendations given by the Eurocode 8: Part 3 (2005) ($1.07 \frac{h_0}{l}$ (%) for flexure and 0.53% for shear) and ASCE/SEI 7-16 (2017) (0.7%). In fact, Figure 10 also displays the maximum allowable drift for masonry shear walls (the most restrictive criteria) which appears to be much higher than the recorded drift of the studied building, indicating that the building complies with the recommendations.

In addition, an equivalent bilinear response of the multi-degree-of-freedom (MDOF) system is calculated according to OPCM 3431/05 (2005) and presented in Figure 11. The overstrength factor Ω (ratio between the elastic strength (V_{el}), which is accepted as crack initiation strength, and (plastic) peak strength (V_u or V_y) of the building has been computed as 1.3 in the positive direction. The value obtained is compatible with the range of 1.2 to 3.8 for two and three storey URM buildings (Morandi and Magenes 2008). Finally, the prediction of the total (plastic) drift $\delta_{pl, pre}$ based on the elastic drift (δ_{el}) and the amplification factor C_d , here taken equal to 1.75 which corresponds to classically unreinforced masonry with detailed plan (ASCE/SEI 7-16 2017). The predicted drift $\delta_{pl, pre}$ is estimated to 0.035% (1.03 mm) which is much smaller than the actual drift at the peak $\delta_{Vmax, exp}$ (Figure 11). This indicates that for this building, the amplification factor provides a conservative estimate of the real full capacity (actual drift) of the building.

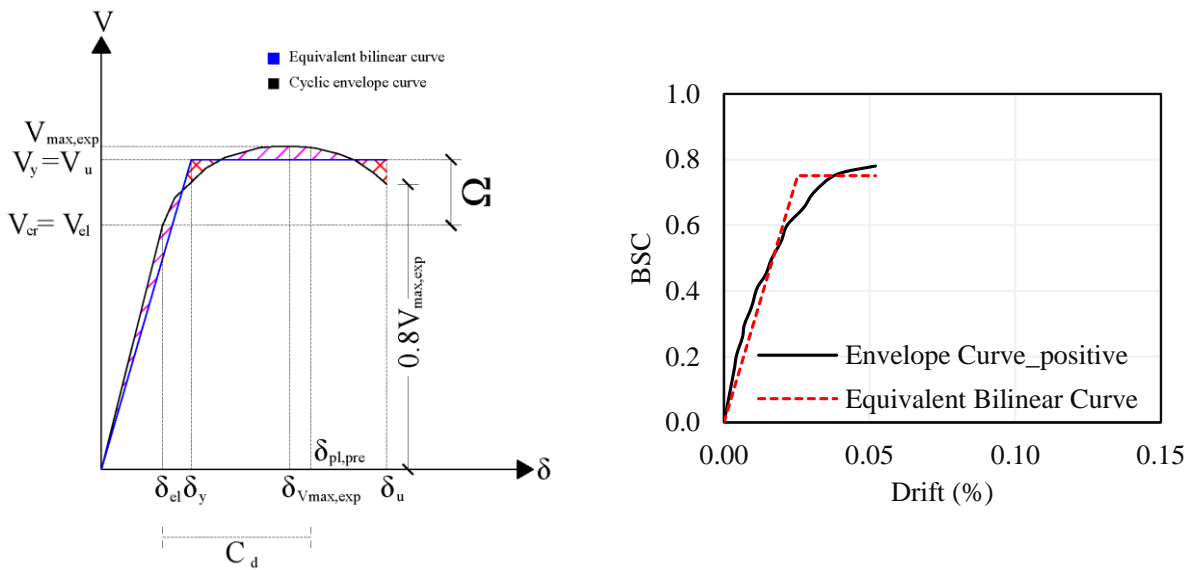


Figure 11. An equivalent bilinear response of the MDOF system

The first evidence of uplifting was observed at the load level of 60% of the total weight of the structure applied in the negative direction. The structure initially uplifts at the base of the intersection of the south and west walls (see Figure 1), then progresses further with the increase of the load level. However, there is an LVDT located next to the door opening at the west façade, as seen in Figure 12. Therefore, displacement has been monitored quantitatively at this point. The uplift is also noticed at the North façade of the setback. Furthermore, the structural walls at the same alignment experience uplift, and the base of the walls is detached from the RC slab. Figure 12 illustrates that the uplift reaches the maximum at the peak base shear (75% of the weight).

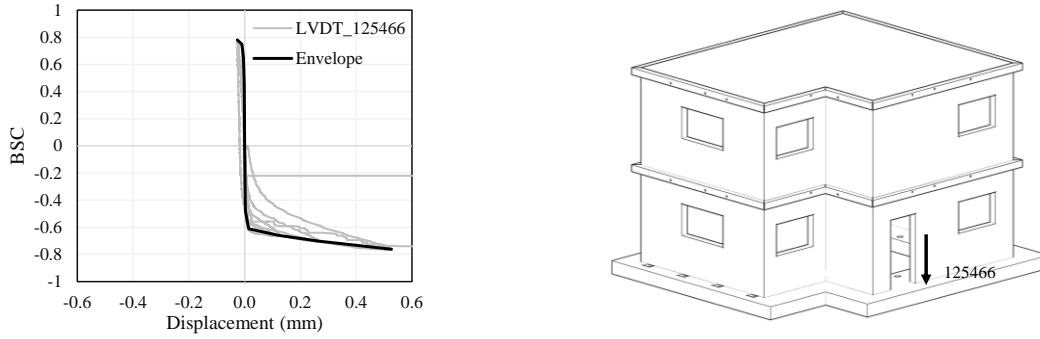


Figure 12. Capacity diagram of the uplift at LVDT 125466

Figure 13 illustrates the crack pattern at the end of 75% of the load application (peak force). Crack initiation occurs at the bed and head joints of the mortar once the lateral load reaches 60% of the total weight of the structure. The first flexural cracks have been discovered in the front pier (north façade). Additionally, horizontal cracks in the out-of-plane direction walls are noted. Accordingly, the uplift starts to dominate the response under the lateral loading in the negative direction once the lateral load exceeds 70% of the total weight. At the end of the experiment, the structural walls have been severely detached from the foundation on the first floor and the slab on the second floor. Furthermore, moderate diagonal cracks also occur at the last load cycle. Up to peak loading, the structural response is mainly governed by the uplifting of the complete structure.

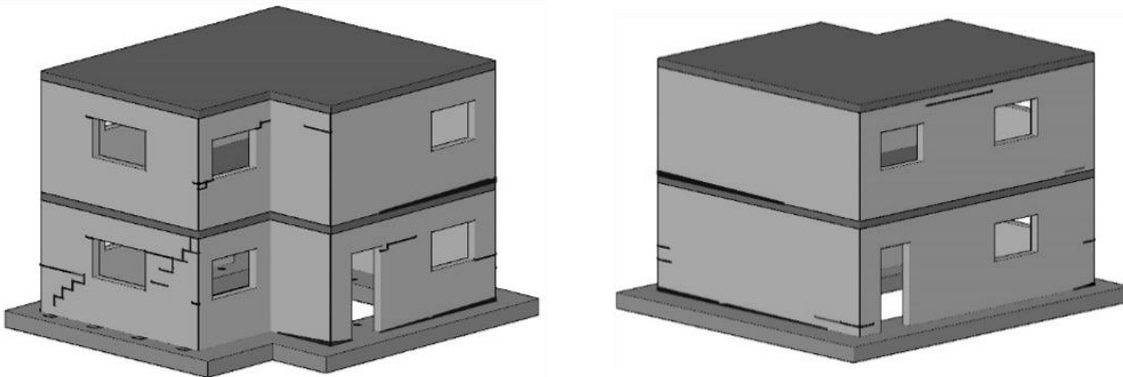


Figure 13. Crack distribution at the end of 75% of the load application

To complement the visual analysis presented before, the images acquired by the camera were analysed using the “ncorr” plugin available in Matlab (2021) (Harilal and Ramji 2014; Blaber et al. 2015). Briefly, the first image is chosen as a reference and then each image is analyzed compared to the first one. Each pixel is transferred to gray level, resulting in a 5472x3648 matrix for each picture. The image is then divided into facets (i.e. points) whose size was chosen to equal 25 pixels (i.e. 23 mm) here. Each facet is finally tracked through the steps, thanks to its unique black-and-white pattern. Post-processing allows displaying the displacement and strain maps of the monitored façade. Figure 14 shows the vertical strain maps at two different instants. Firstly, DIC analysis unveiled that the first cracks in the building occurred in the negative loading direction, at approximately 50% of the total weight (Figure 14a). They are located on the right pier of each story at the window level, though more noticeable in the first one. At the final stage of the experiments (Figure 14b), the tensile cracks are much more visible, and almost cover the entire width of the right piers. Additionally, a stepped crack has been also observed in the left pier of the first story, and

horizontal cracks are noticeable at the top of the two storeys. One can note that these cracks delimitate rocking macro-blocks. However, the latter did not develop entirely and did not drive the structural failure, as the building uplift has been activated before.

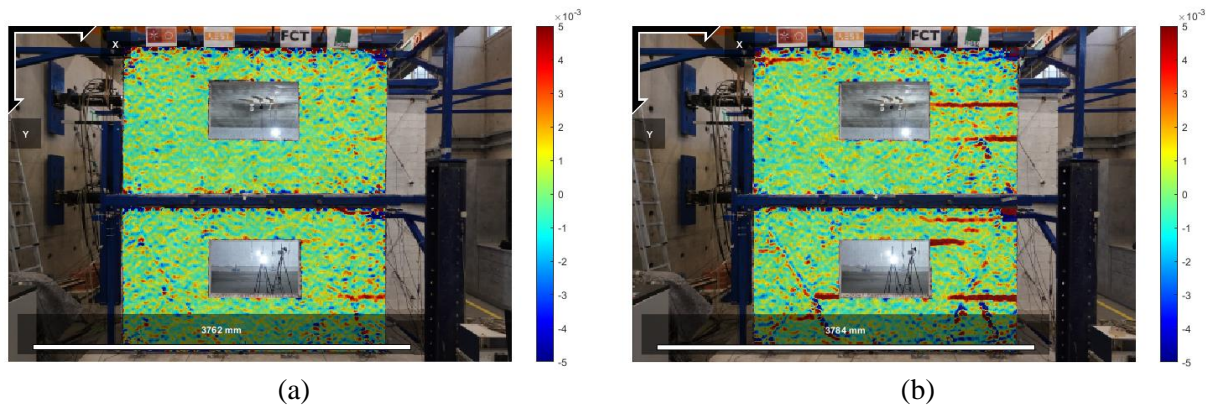


Figure 14. Vertical strain maps obtained after (a) 50% of the total weight and (b) 75% of the total weight.

5 Conclusions

In this paper, an unreinforced two-story masonry building with an irregular plan is investigated using a cyclic quasi-static test. Additionally, dynamic identification of the structure has carried out by performing ambient vibration measurements and operational modal analysis. According to the observations made during the test, the experimental setup and the post-tensioned tie-rods ensures uniform distribution of loads during pushing and pulling. The lateral load capacity of the irregular building is nearly the same for both positive and negative directions. However, higher deformation capacity is noted in the negative transversal direction which could be associated with the domination of the uplift in the response for that direction. In terms of damage, the first flexural cracks have been unveiled on the North façade thanks to DIC at 50% of the total weight. Then, flexural cracks intensified at the piers on the North façade of the building. Various horizontal cracks are also discovered, which could be related to the torsional effect. At 75% of the total weight of the structure, the structure reaches the maximum capacity primarily due to the rocking of the entire structure and the detachment of the base of the walls from the foundation.

Acknowledgments

This work is financed by national funds through FCT - Foundation for Science and Technology, under grant agreement SFRH/BD/143949/2019 attributed to the 1st author. Additionally, this work is financed by national funds through FCT - National Foundation for Science and Technology, in the scope of the research project “Experimental and Numerical Pushover Analysis of Masonry Buildings (PUMA)” (PTDC/ECI-EGC/29010/2017).

References

- Aldemir A, Binici B, Canbay E, Yakut A (2017) Lateral load testing of an existing two story masonry building up to near collapse. *Bull Earthq Eng* 15:3365–3383. <https://doi.org/10.1007/s10518-015-9821-3>
- ARTEMIS Modal v.6.0 SVS-Structural Vibration Solutions A/S
- ASCE/SEI 7-16 (2017) Minimum design loads and associated criteria for buildings and other structures
- Aşıkoğlu A, Del Re A, Vasconcelos G, Lourenço PB (2021) Quasi-Static Test on a Half-Scale Two-Story

- Urm Building : Quasi-Static Test on a Half-Scale Two-Story Urm Building : Mechanical Characterization of. In: Capela C, Ruben RB, Belt MS, et. al. (eds) 12th National Congress on Experimental Mechanics. Monte Real, pp 1–14
- Aşıkoğlu A, Vasconcelos G, Lourenço PB, Pantò B (2020) Pushover analysis of unreinforced irregular masonry buildings: Lessons from different modeling approaches. *Eng Struct* 218:. <https://doi.org/10.1016/j.engstruct.2020.110830>
- Avila L, Vasconcelos G, Lourenço PB (2018) Experimental seismic performance assessment of asymmetric masonry buildings. *Eng Struct* 155:298–314. <https://doi.org/10.1016/j.engstruct.2017.10.059>
- Azizi H (2018) Analytical and empirical seismic fragility analysis of irregular URM buildings with box behavior. University of Minho
- Blaber J, Adair B, Antoniou A (2015) Ncorr: Open-Source 2D Digital Image Correlation Matlab Software. *Exp Mech* 55:1105–1122. <https://doi.org/10.1007/s11340-015-0009-1>
- Caddemi S, Calì I, Cannizzaro F, Pantò B (2017) New frontiers on seismic modeling of masonry structures. *Front Built Environ* 3:1–16. <https://doi.org/10.3389/fbuil.2017.00039>
- Calì I, Marletta M, Pantò B (2012) A new discrete element model for the evaluation of the seismic behaviour of unreinforced masonry buildings. *Eng Struct* 40:327–338. <https://doi.org/10.1016/j.engstruct.2012.02.039>
- Candeias PX, Campos Costa A, Mendes N, et al (2017) Experimental Assessment of the Out-of-Plane Performance of Masonry Buildings Through Shaking Table Tests. *Int J Archit Herit* 11:31–58. <https://doi.org/10.1080/15583058.2016.1238975>
- Dolce M, Ponzo FC, Goretti A, et al (2008) 3D Dynamic Tests on 2 / 3 Scale Masonry Buildings Retrofitted With Different Systems. *Proc 14th World Conf Earthq Eng*
- Drysdale RG, Hamid AA (2008) *Masonry Structures Behavior and Design*, 3rd edn. The Masonry Society
- EN 1998-3:2005 EN 1998-3: Eurocode 8: Design of structures for earthquake resistance – Part 3: Assessment and retrofitting of buildings
- Eurocode 6 (2018) Eurocode 6 - Design of masonry structures - Part 1-1: General rules for reinforced and unreinforced masonry structures
- Ghiassi B, Xavier J, Oliveira D V., Lourenço PB (2013) Application of digital image correlation in investigating the bond between FRP and masonry. *Compos Struct* 106:340–349. <https://doi.org/10.1016/j.compstruct.2013.06.024>
- Ghorbani R, Matta F, Sutton MA (2015) Full-Field Deformation Measurement and Crack Mapping on Confined Masonry Walls Using Digital Image Correlation. *Exp Mech* 55:227–243. <https://doi.org/10.1007/s11340-014-9906-y>
- Graziotti F, Tomassetti U, Kallioras S, et al (2017) Shaking table test on a full scale URM cavity wall building. *Bull Earthq Eng* 15:5329–5364. <https://doi.org/10.1007/s10518-017-0185-8>
- Harilal R, Ramji M (2014) Adaptation of Open Source 2D DIC Software Ncorr for Solid Mechanics Applications. *9th Int Symp Adv Sci Technol Exp Mech* 1–6
- Jaiswal KS, Wald DJ (2008) *Creating a Global Building Inventory for Earthquake Loss Assessment and Risk Management: U.S. Geological Survey Open-File Report*. 1160:113
- Kallioras S, Guerrini G, Tomassetti U, et al (2018) Experimental seismic performance of a full-scale unreinforced clay-masonry building with flexible timber diaphragms. *Eng Struct* 161:231–249. <https://doi.org/10.1016/j.engstruct.2018.02.016>
- Lagamarsino S, Penna A, Galasco A (2006) TREMURI program: seismic analysis program for 3D masonry buildings. Univ Genoa
- Lourenço P., Marques R (2020) Design of masonry structures (General rules): Highlights of the new European masonry code. In: Kubica, Kwiecien, Bednarz (eds) *Brick and Block Masonry - From*

Historical to Sustainable Masonry. Taylor & Francis, Krakow

- Magenes G, Calvi GM, Kingsley G (1995) Seismic Testing of a Full-scale, Two-story Masonry Building: Test Procedure and Measured Experimental Response
- Magenes G, Penna A, Senaldi IE, et al (2014) Shaking table test of a strengthened full-scale stone masonry building with flexible diaphragms. *Int J Archit Herit* 8:349–375. <https://doi.org/10.1080/15583058.2013.826299>
- Matlab (2021) Matlab user's guide
- Mazon N, Valluzzi MR, Aoki T, et al (2009) Shaking Table Tests on Two Multi-leaf Stone Masonry Buildings. 11th Can Mason Symp
- Mendes N (2012) Seismic Assessment of Ancient Masonry Buildings : Shaking Table Tests and Numerical Analysis. University of Minho
- Morandi P, Magenes G (2008) Seismic design of masonry buildings: current procedures and new perspectives. 14th World Conf Earthquake Eng
- OPCM 3431/05 (2005) Primi elementi in materia di criteri generali per la classificazione sismica del territorio nazionale e di normative tecniche per le costruzioni in zona sismica: G.C. No. 105 and G.C. No. 107 (in Italian).
- Rajaram S, Vanniamparambil PA, Khan F, et al (2017) Full-field deformation measurements during seismic loading of masonry buildings. *Struct Control Heal Monit* 24:1–14. <https://doi.org/10.1002/stc.1903>
- Shahzada K, Khan AN, Elnashai AS, et al (2012) Experimental seismic performance evaluation of unreinforced brick masonry buildings. *Earthq Spectra* 28:1269–1290. <https://doi.org/10.1193/1.4000073>
- Tomažević, M., Lutman, M., & Weiss P (1996) Seismic upgrading of old brick-masonry urban houses: Tying of walls with steel ties.